Reports

Spectral Reflectance Properties of Hydrocarbons: Remote-Sensing Implications

EDWARD A. CLOUTIS

The spectral reflectance properties of bituminous tar sands were examined in the wavelength range from 0.35 to 2.6 micrometers. Unique absorption features due to all the major phases, except quartz, appear in the spectra. The intensities of the absorption features correlate with the abundances of the various phases. The results of this study have applications to the remote sensing of many terrestrial and extraterrestrial targets because of potential similarities between tar sand and other hydrocarbon occurrences. For example, it is found that highly polymerized hydrocarbons are a plausible constituent of the dark material on one of Saturn's satellites, Iapetus.

A SYSTEMATIC STUDY OF THE SPECTRAL reflectance properties of bituminous tar sands was undertaken in order to determine whether this class of materials has distinct spectral properties (*1*). Tar sands are composed of a mixture of clays, bitumen (a complex array of variously polymerized hydrocarbons), quartz grains, water, and minor accessory minerals (*2–4*). Understanding the spectral properties of this material is essential for geological remote sensing of terrestrial and extraterrestrial targets, because very little is known about the spectral reflectance properties of hydrocarbon-bearing materials.

Among the leading extraterrestrial candidates for possible hydrocarbon occurrences are Trojan asteroids, cometary nuclei, and the dark side of one of Saturn's satellites, Iapetus (*5, 6*). Tar sands may serve as reasonable spectral analogs of these objects and other bodies whose surfaces are believed to be composed of various combinations of organic matter, clays, and H_2O. Spectral analysis of the tar sands may also make possible the remote-sensing detection of terrestrial, surficial hydrocarbon seeps, because highly polymerized hydrocarbons are characteristic of both tar sands and surface exposures (*7*). The term kerogen is often used to refer to extraterrestrial occurrences of hydrocarbons. Kerogen and bitumen differ primarily in the hydrogen/carbon ratio; in bitumen the ratio is higher because of greater maturation (*7*). Rapid characterization of tar sands and heavy oil samples would be possible with the development of quantitative spectral analysis techniques. This could improve commercial bitumen extraction efficiencies and simplify the onerous procedures now required for tar sand characterization. Spectral reflectance techniques may eventually be extended to the analysis of other nonrenewable energy resources such as oil shales and coals.

All the phases present in the Athabasca tar sands, except quartz, display distinct absorption bands that are potentially resolvable. The shapes, intensities, and wavelength positions of these bands may provide information on the physical and chemical properties of the various phases (*8–11*).

Many organic compounds display electronic transitions arising from excitations of bonding electrons in the wavelength region from 0.1 to 0.35 μm. As the complexity of the organic molecules increases, the maximum absorption shifts toward longer wavelengths and individual bands become less distinct because of increasing overlap (*12–14*). A material as complex as bitumen is not expected to exhibit individual, resolvable absorption bands in the ultraviolet and visible spectral region. A broad overall reflectance decrease toward shorter wavelengths is seen in coals, chars, oil shales, and tar sands (*12, 14–17*).

The wavelength positions of the most intense, major organic fundamental bands are listed in Table 1. Because the energies of the fundamental absorption bands depend on a number of factors such as local atomic configurations (*18*), the wavelength positions of the overtone and combination bands are somewhat uncertain (Table 2). The low overall reflectance of tar sands is expected to suppress all but the most prominent of these bands. The most promising regions in which to search for organic absorption bands are near 1.7 μm and between 2.2 and 2.6 μm (*16, 19*). The 1.7-μm region is dominated by various C–H stretching overtones and combination bands. The fundamental bands that contribute to this feature are the most intense absorbers in the infrared spectra of bitumen (*20*). The region from 2.2 to 2.6 μm is affected by numerous overlapping combination and overtone bands. Bitumen transmission spectra show moderately intense absorption between ~1750 and ~900 cm^{-1}, which can combine in a number of ways in the region from 2.2 to 2.6 μm (*2, 12, 20, 21*). Because of the sheer number of possible bands, the region has a low overall reflectance with only the most intense absorption bands being partially resolvable (*14, 15, 22*).

Transition series elements, particularly vanadium and nickel, complexed with porphyrin-type molecules are quite common in the

Table 1. Positions of the major organic fundamental absorption bands in energy space.

Band	Fundamental frequency (cm^{-1})	Assignment
a	3030	Alkene, aromatic C–H stretch
b	2950	Asymmetric CH_3 stretch
c	2920	Asymmetric CH_2 stretch
d	2875	Symmetric CH_3 stretch
e	2850	Symmetric CH_2 stretch
f	1700	Carbonyl-carboxyl C–O stretch
g	1600	Aromatic carbon stretch
h	1450	Asymmetric CH_2, CH_3 bend
i	1375	Symmetric CH_3 bend

Table 2. Predicted wavelength positions of the most intense overtones and combinations of the major fundamental organic absorption bands listed in Table 1.

Combination-overtone band	Wavelength (μm)
2a	1.65
a + c	1.68
2b	1.69
a + e	1.70
2c	1.71
b + d	1.72
c + e	1.73
2d	1.74
2e	1.75
e + f	2.20
c + g	2.21
e + g	2.25
b + h	2.27
c + h	2.29
b + i, d + h	2.31
e + h	2.33
d + i	2.35
c + j	2.53

Department of Geology, University of Alberta, Edmonton, Alberta, Canada T6G 2E3.

Downloaded from www.sciencemag.org on December 5, 2013

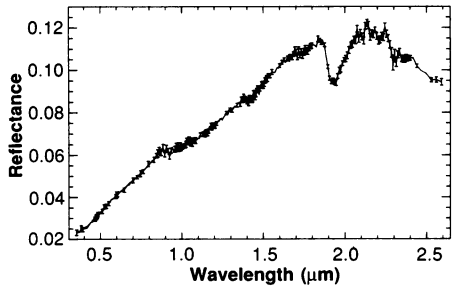

Fig. 1. Reflectance spectrum (0.35 to 2.6 μm) of a low-bitumen tar sand (sample 82-05) (*1*).

asphaltic fraction of tar sands. They display a number of absorption bands in the ultraviolet and visible spectral regions. The most intense of these occurs at ~0.4 μm and has been detected in the spectra of oil shale and carbonaceous chondrites (*23*).

The bitumen content in the Athabasca tar sands typically ranges from 0 to 15% by weight (*3*). This range was arbitrarily divided into three 5% intervals in order to display spectral variations as a function of changing phase abundances. The reflectance spectra of low-, medium-, and high-bitumen samples were measured, and a representative sample of each group was selected for more detailed analysis.

The low-bitumen group is characterized by prominent absorption bands due to the clays (Fig. 1). The absorption bands at ~1.4, 1.9, 2.2, and 2.3 to 2.6 μm are assigned to structural and adsorbed water in the clays and to cation–OH vibrational bands (*8*). The wavelength position of the 1.9 μm band (1.92 μm) does not coincide with that expected for free water [1.94 μm (*11*)]. The broadness of this band and the 1.4-μm band is consistent with the presence of water in a variety of sites or with structurally disordered clays (*2*). The decrease in reflectance from 2.3 to 2.6 μm is also characteristic of a clay-dominated spectrum (*8*). Discrete bitumen absorption bands are weak or absent in spite of the amount of bitumen present (3.2%) and the dark appearance of the sample. Indirect evidence for bitumen comes from the low overall reflectance of the sample, which is not characteristic of most clays (*8, 9*).

Spectra of medium-bitumen samples are richer in detail than those of the low-bitumen samples and differ in other ways. The depth of the 1.9 μm band is reduced, a new band appears at ~1.7 μm, the depth of the band in the region from the 2.3 to 2.6 μm is greater (Table 3), and the overall reflectance slope in this range is slightly positive (Fig. 2). The absorption band that appears at 1.7 μm can be attributed to first-order overtones and combinations of the various C–H stretching fundamentals (Tables 1 and 2). The increase in absorption in the region from 2.3 to 2.6 μm is also a manifestation of the increasing bitumen content. The slightly positive slope in this region is not characteristic of clays, which show a negative slope. This suggests that bitumen is overriding the spectral signature of the clays in this region.

Table 3. Wavelength positions of the observed absorption bands and their depths, D_b. Some band positions are given as ranges because of variations between different sample spectra.

Band minimum (μm)	Sample		
	82-05	87-04	86-19
0.40	7.0		
1.39–1.41	4.5	6.0	3.0
1.72–1.75	1.8	9.9	18.6
1.92–1.95	19.0	10.4	3.8
2.10	5.0		
2.15–2.18	4.1	9.6	11.4
2.21	6.5	15.5	14.3
2.31	14.8	40.2	54.3
2.35	13.9	38.9	55.0
2.45	16.9	35.6	47.9
2.55	22.1	33.9	38.6

Spectra of samples with high bitumen content are dominated by bitumen (Fig. 3), the second most abundant phase after quartz in these samples (Table 3). All the major absorption bands can be attributed to hydrocarbons. The expected clay-water bands at 1.4 and 1.9 μm are virtually absent. The 1.7-μm bitumen absorption region is very prominent, and its nonsymmetrical shape is consistent with multiple, overlapping C–H absorption bands. The absorption is strong in the region from 2.3 to 2.6 μm and has a positive slope, neither of which is characteristic of clays. The absorption band at 2.3 μm is very intense, and the positive slope in the region from 2.3 to 2.6 μm is the result of the dominance of this feature.

Each spectral group, divided on the basis of bitumen content, exhibits unique spectral properties. These variations can be related to the physical and chemical properties of the samples that have been independently determined. Bitumen and clay abundances are generally inversely correlated. There is no simple correlation between spectral albedo and any of the major phase abundances. The same holds true for the abundances of quartz versus clay. Bitumen and quartz abundances are positively correlated. Spectra corresponding to samples with high and low bitumen contents are dominated by hydrocarbon and clay absorption features, respectively.

The most prominent absorption band attributable to the various forms of water is present near 1.9 μm and is most intense in the most water- and clay-rich samples (Table 4). This wavelength region is useful for clay-water determination because, unlike the region from 2.3 to 2.6 μm, it is not significantly overlapped by hydrocarbon absorptions. The broadness and complex shape of the 1.9-μm band is consistent with the presence of water in a number of sites in the clay, structurally disordered clays, or more than one species of clay. All three interpretations are borne out by independent studies of the Athabasca clays (*2, 3*). There may be a moderate contribution by free water at 1.94 μm, but its presence cannot be unambiguously resolved.

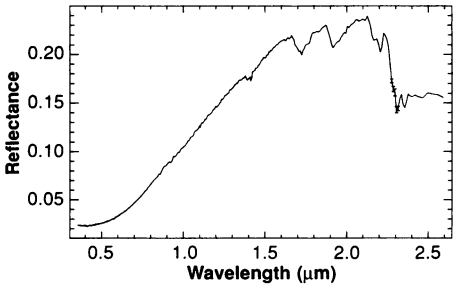

Fig. 2. Reflectance spectrum (0.35 to 2.6 μm) of a medium-bitumen tar sand (sample 87-04).

The absorption band near 1.4 μm is most prevalent in the low-bitumen content spectra and is assigned to structural and bound water in the clays. The available spectral information on various forms of water shows that free water and polymerized water absorb at different wavelengths (>1.45 μm) than water in clays (1.38 to 1.42 μm). The broadness of this band is interpreted in the same way as that of the 1.9-μm band (*24*).

Clay lattice–OH absorption bands are expected in the region from 2.2 to 2.6 μm. This band is unexpectedly weakest in the spectrum of the most clay-rich sample (Fig. 1). The highly absorbing nature of bitumen in this region, and its low abundance in the clay-rich samples, explains this discrepant behavior. Clay spectra normally exhibit high overall reflectance (*8, 9*). The low-bitumen spectrum (Fig. 1) contains 28% clay-sized particles and shows only clay absorption bands but has a very low overall reflectance. The low reflectance may be caused by the presence of the bitumen, iron oxide contaminants, or transition series element substitutions (*3*). A reflectance spectrum of a transition element–bearing clay, glauconite (Fig. 4), shows a number of similarities to the clay-rich spectrum of Fig. 1: a concave reflectance rise between 0.9 and 1.5 μm, a weak or absent 1.4-μm absorption band, and a reflectance decrease beyond 2.3 μm. The overall reflectance of the glauconite is still significantly higher than that of the most clay-rich sample (Fig. 1). Even though transition series–bearing clays may be present, glauconite itself has not been identified in Athabasca tar sands (*2, 3*). The spectrum of the low-bitumen sample is consistent

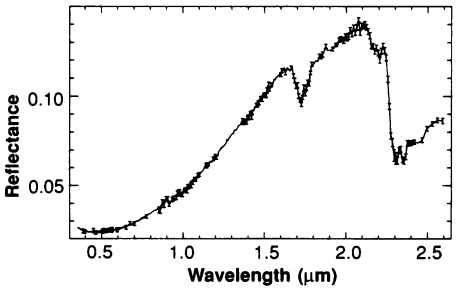

Fig. 3. Reflectance spectrum (0.35 to 2.6 μm) of a high-bitumen tar sand (sample 86-19).

with a cation-substituted clay but requires the presence of a phase with low overall reflectance. Bitumen seems the likeliest candidate for the darkening material.

The high-bitumen spectrum corresponds to a sample with 5% clay-sized particles and has a virtually undetectable 1.9-μm clay-water band. Thus a lower limit of ~5% can be placed on spectral determination of clays in organic-rich materials of this type. Bitumen serves as an effective suppressor of what are normally, moderately intense absorption bands.

The regions at 1.7 and 2.3 to 2.6 μm are the best areas for the detection of various C–H absorption bands. The 1.7-μm region is preferable because it is not overlapped by clay and water absorption bands and is the most recognizable feature shortward of 2.1 μm. The complex shape of this band is consistent with the presence of multiple, partially overlapping absorption bands, although no attempt has yet been made to deconvolve this feature into its constituent bands. The use of this absorption feature places a lower detection limit of ~4% on bitumen abundances in tar sands.

The near absence of a 1.9-μm clay-water band in Fig. 3 strongly suggests that this spectrum is a good representative of polymerized hydrocarbons plus spectrally neutral material. The moderate-strength absorption bands that appear in all the sample spectra between 2.17 and 2.25 μm can best be assigned to both clay lattice–OH and organic bands, because there is no simple correlation between their band depths and any one phase abundance. The overall slope of the region from 2.3 to 2.6 μm is sensitive to both bitumen and clay contents. Clays consistently exhibit a negative slope in this region [see (*8, 9*) and Fig. 4], whereas organic materials show a positive slope (*15, 16, 22*). The changeover from negative to positive slope occurs in the medium-bitumen group.

Changes in bitumen content affect the ultraviolet and visible spectral regions. The point of minimum reflectance shifts to longer wavelengths as the bitumen content increases. The wavelength position of the reflectance minimum in Fig. 3 is ~0.47 μm, which corresponds to an average of six condensed aromatic rings per molecule if we use the calibration of Badger (*25*). This is in good agreement with the conventional analytical results of five rings per molecule for the resin fraction, the most abundant organic group (*3, 20*). The shape of the reflectance spectrum between 0.5 and 1.5 μm changes from two linear segments with a slope break at ~0.9 μm to a smoother concave slope with increasing bitumen and decreasing clay contents. The former shape is similar to that of the glauconite spectrum (Fig. 4); the latter shape is consistent with a continuum of charge-transfer energy levels expected in complex hydrocarbons.

Table 4. Phase abundances of the samples (in percentages by weight).

Sample	Abundances (%)			<400 mesh (%)	>400 mesh (%)
	Bitumen	Water	Solids		
82-05	3.2	8.1	88.7	32.1	67.9
87-04	8.1	6.6	85.3	29.3	70.7
86-19	13.2	2.5	83.9	6.0	94.0

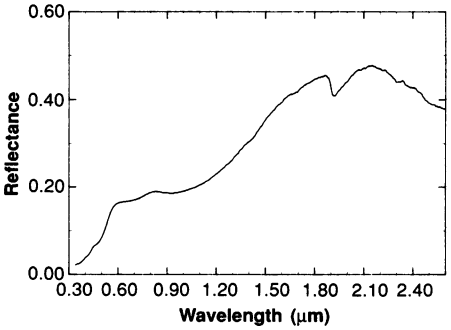

Fig. 4. Reflectance spectrum (0.35 to 2.6 μm) of glauconite, which has a number of similarities to the Iapetus dark material.

The intense Soret band, which is characteristic of porphyrins, should be present at ~0.4 μm (*23*). The low overall reflectance of the sample spectra makes identification of this feature very difficult, and its unambiguous presence has not yet been established.

Hydrocarbons are suspected to be present on a number of extraterrestrial bodies (*5, 6*) and have been found in carbonaceous chondrites (*26*). Iapetus was selected for more detailed spectral analysis. One hemisphere is almost entirely covered with a very dark substance of unknown composition. Earlier investigators used a mixing model to remove the spectral signature of water ice and isolate the dark material (*6*), which shows a gradual rise in reflectance toward longer wavelengths with only minor absorption bands. If the removal procedure for the water ice signature did not inadvertently delete additional features, there is no evidence for any of the expected organic absorption bands. In particular, the regions at 1.7 and 2.3 to 2.6 μm show none of the characteristics of highly polymerized hydrocarbons.

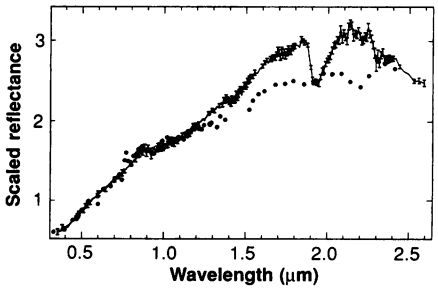

Fig. 5. Normalized reflectance spectrum of the low-bitumen tar sand sample with the telescopic spectral data for the Iapetus dark material from (*6*) overlain (filled circles).

The best match to the dark material was found to be a mixture of 90% clay and 10% coal tar representing organic matter (*6*). The low-bitumen sample (Fig. 1) consists of the same ratio of clay to organics and, like its coal tar counterpart, is free of detectable organic absorption bands. The clay–coal tar spectrum provides a good match to the overall change in reflectance with wavelength of the Iapetus spectrum, although the fit to the region from 0.8 to 1.4 μm is not very good. The low-bitumen spectrum (normalized to match the Iapetus dark material) provides a much better fit to the region from 0.8 to 1.4 μm and also shows a change in slope at ~0.9 μm (Fig. 5). Beyond 1.4 μm the reflectance of the tar sand is consistently higher than that of the Iapetus dark material; the clay absorption bands at 1.9 μm and 2.2 to 2.5 μm are also much more intense in the tar sand spectrum.

Neither the clay–coal tar mixture nor the tar sand are perfect spectral matches to the Iapetus dark material. The reflectance spectrum of glauconite (Fig. 4) exhibits a number of desirable spectral features for matching with the Iapetus dark material. The difference between the minimum and maximum reflectance is comparable to that found for the dark material, the slope break at ~0.9 μm is present, and a weak 1.9-μm clay-water band is present. Most other clays do not show the same reflectance difference between minimum and maximum reflectance (*8*), because they contain only minor amounts of transition series elements. A dark material must be added to this spectrum to further suppress the 1.9-μm band and neutralize the reflectance dropoff beyond 2.2 μm.

No one of the sample spectra is a perfect match to the Iapetus dark material. Because each material examined has certain desirable spectral characteristics, a complex, intimate mixture of different materials may be required. An iron-substituted clay seems to be

a necessary constituent (*5*). The presence of some amount of a highly polymerized hydrocarbon, like the bitumen present in tar sands, may be needed to modify the clay spectrum in the region from 0.8 to 1.4 μm. A few percent of bitumen can be present and not exhibit distinct absorption bands. Finally, a material spectrally similar to the coal tar extract is needed, which can effectively mask the negative slope of the clays between 2.2 and 2.6 μm, reduce the reflectance rise at longer wavelengths, and suppress clay-organic bands at 2.2 to 2.6 μm.

REFERENCES AND NOTES

1. The tar sand samples used in this study are from the Athabasca deposit in northeastern Alberta and consist of viscous organic matter embedded in clastic sediments of the Cretaceous McMurray and Clearwater formations [B. Nagy and G. C. Gagnon, *Geochim. Cosmochim. Acta* **23**, 155 (1961)]. They were obtained from the Alberta Oil Sands Technology and Research Authority [(AOSTRA), Edmonton, Alberta] Oil Sands Sample Bank, along with some analytical data. The reflectance spectra were acquired at the U.S. Geological Survey spectrometer facility in Denver, CO, and the National Aeronautics and Space Administration Reflectance Experiment Laboratory (RELAB) spectrometer facility at Brown University in Providence, RI. Comprehensive descriptions of the instruments and data-processing procedures are available in the following references: R. N. Clark, *Publ. Astron. Soc. Pac.* **92**, 221 (1980); C. M. Pieters, *J. Geophys. Res.* **88**, 9534 (1983); T. V. V. King and W. I. Ridley, *ibid.* **92**, 11457 (1987). The homogeneity of the tar sand samples could only be assessed visually. The samples were gently chopped and mixed until a visually uniform mixture resulted. They were then placed in sample holders and lightly compressed to provide a flat surface for spectral measurement. All samples were measured relative to Halon. The tar sand spectra were acquired with the use of an integrating sphere arrangement at the U.S. Geological Survey facility. The glauconite was spectrally characterized in a bidirectional reflectance mode at the NASA RELAB facility, using an incidence angle of 0° and an emission angle of 15°. A duplicate tar sand spectrum, acquired to check for reproducibility, was within the error limits of the data. The error bars in the spectral data represent 1 SD of the mean. Band depth (D_b), used extensively in spectral analysis, is here defined as

$$D_b = 1 - R_b/R_c$$

where R_c is the reflectance of a straight-line continuum at the wavelength position of a reflectance minimum and R_b is the minimum reflectance at the same wavelength. The continuum was constructed as a straight line tangent to the spectrum on either side of the absorption feature of interest. The continuum for the region from 2.3 to 2.6 μm was taken as a horizontal line tangent to the reflectance maximum near 2.2 μm.
2. E. Czarnecka and J. E. Gillot, *Clays Clay Miner.* **28**, 197 (1980); T. M. Ignasiak *et al.*, *Fuel* **62**, 353 (1983).
3. J. A. Bichard, *Oil Sand Composition and Behaviour Research* (AOSTRA Technical Publication Series 4, Edmonton, Alberta, Canada, 1987).
4. M. L. Selucky *et al.*, *Fuel* **56**, 369 (1977); J. W. Bunger *et al.*, *ibid.* **58**, 183 (1979).
5. J. Gradie and J. Veverka, *Nature* **283**, 840 (1980); C. Chyba and C. Sagan, *ibid.* **330**, 350 (1987); E. K. Jessberger, A. Christoforidis, J. Kissel, *ibid.* **332**, 691 (1988); D. P. Cruikshank and R. H. Brown, *Science* **238**, 183 (1987).
6. D. P. Cruikshank *et al.*, *Icarus* **53**, 90 (1983); J. F. Bell *et al.*, *ibid.* **61**, 192 (1985).
7. J. M. Hunt, *Petroleum Geochemistry and Geology* (Freeman, San Francisco, 1979).
8. G. R. Hunt and J. W. Salisbury, *Mod. Geol.* **1**, 283 (1970); ———, C. J. Lenhoff, *ibid.* **4**, 85 (1973); G. R. Hunt, *Geophysics* **42**, 501 (1977); R. N. Clark, *J. Geophys. Res.* **86**, 3074 (1981); T. V. V. King, thesis, University of Hawaii (1986).
9. J. D. Lindberg and D. G. Snyder, *Am. Mineral.* **57**, 485 (1972); S. C. Feldman, J. V. Taranik, D. A. Mouat, in *Proceedings of the Airborne Imaging Spectrometer Data Analysis Workshop*, G. Vane and A. F. H. Goetz, Eds. (Jet Propulsion Laboratory, Pasadena, CA, 1985), p. 56; G. Vane and A. F. H. Goetz, *Remote Sensing Environ.* **24**, 1 (1988); S. A. Drury and G. A. Hunt, *Photogramm. Eng. Remote Sensing* **54**, 1717 (1988); C. M. Pieters and J. F. Mustard, *Remote Sensing Environ.* **24**, 151 (1988).
10. J. E. Zajic, D. G. Cooper, J. A. Marshall, D. F. Gerson, *Fuel* **60**, 619 (1981); K. Buijs and G. R. Choppin, *J. Chem. Phys.* **39**, 2035 (1963); H. Yamatera, B. Fitzpatrick, G. Gordon, *J. Mol. Spectrosc.* **14**, 268 (1964); M. R. Thomas *et al.*, *J. Phys. Chem.* **69**, 3722 (1965); K. B. Whetsel, *Appl. Spectrosc. Rev.* **2**, 1 (1968); J. D. Worley and I. M. Klotz, *J. Chem. Phys.* **45**, 2868 (1966).
11. J. G. Bayly, V. B. Kartha, W. H. Stevens, *Infrared Phys.* **3**, 211 (1963); R. Goldstein and S. S. Penner, *J. Quant. Spectrosc. Radiant. Transfer* **4**, 441 (1964).
12. M. L. Boyd and D. S. Montgomery, *J. Inst. Pet. London* **49**, 345 (1963).
13. B. E. Hudson, Jr., R. F. Robey, J. F. Nelson, in *Proceedings of the Fifth World Petroleum Congress* (Fifth World Petroleum Congress, Inc., New York, 1959), vol. V, p. 1; R. M. Silverstein and G. C. Bassler, *Spectrometric Identification of Organic Compounds* (Wiley, New York, 1967).
14. L. A. Gilbert, *Fuel* **39**, 393 (1960).
15. O. Ito, H. Seki, M. Iino, *ibid.* **67**, 573 (1988).
16. W. Kaye, *Spectrochim. Acta* **6**, 257 (1954); R. F. Goddu, *Anal. Chem.* **29**, 1790 (1957); S. A. Fysh *et al.*, *Appl. Spectrosc.* **39**, 354 (1985); N. A. McAskill, *ibid.* **41**, 313 (1987).
17. T. Yokota *et al.*, *Fuel* **65**, 1142 (1986); E. A. Kmetko, *Phys. Rev.* **82**, 456 (1951).
18. G. Svehla, *Comprehensive Analytical Chemistry*, vol. VI, *Analytical Infrared Spectroscopy* (Elsevier, Amsterdam, 1976); P. C. Painter *et al.*, *Appl. Spectrosc.* **35**, 475 (1981); M. P. Fuller *et al.*, *Fuel* **61**, 529 (1982); P. C. Painter *et al.*, *ibid.* **66**, 973 (1987); P. W. Yang *et al.*, *Energy Fuels* **2**, 26 (1988).
19. R. J. Moore, R. J. Gordon, R. C. Eiffert, in *Proceedings of the Fifth World Petroleum Congress* (Fifth World Petroleum Congress, Inc., New York, 1959), vol. V, p. 13.
20. M. L. Boyd and D. S. Montgomery, *Canadian Dep. Mines Tech. Surv. R78* (1961); *Canadian Dep. Mines Tech. Surv. R88* (1961); *Canadian Dep. Mines Tech. Surv. 104* (1962).
21. B. Nagy and G. C. Gagnon, *Geochim. Cosmochim. Acta* **23**, 155 (1961).
22. J. C. Donini and K. H. Michaelian, *Infrared Phys.* **26**, 135 (1986); E. K. Plyler and W. S. Benedict, *J. Res. Natl. Bur. Stand.* **47**, 202 (1951).
23. J. B. F. Champlin and H. N. Dunning, *Econ. Geol.* **55**, 797 (1960); G. W. Hodgson and B. L. Baker, *Chem. Geol.* **2**, 187 (1967); E. W. Funk and E. Gomez, *Anal. Chem.* **49**, 972 (1977); P. N. Holden and M. J. Gaffey, *Meteoritics* **22**, 412 (1987).
24. R. B. Singer and T. L. Roush, *Lunar Planet. Sci. Conf.* **14**, 708 (1983).
25. G. M. Badger, *Structures and Reactions of the Aromatic Compounds* (Cambridge Univ. Press, London, 1957).
26. B. Nagy, *Carbonaceous Meteorites* (Elsevier, Amsterdam, 1975).

27. Supported by a scholarship and research grant from AOSTRA and an American Association of Petroleum Geologists grant-in-aid (582-12-01). I thank D. Wallace and D. Henry of the AOSTRA Oil Sands Sample Bank for providing the tar sand samples. I thank R. Clark and G. Swayze of the U.S. Geological Survey in Denver, C. Pieters and S. Pratt at Brown University for providing access to their respective spectrometer facilities, and M. Gaffey for providing the spectrum analysis programs and encouragement throughout. I am also grateful to two anonymous reviewers for many useful suggestions and corrections.

30 December 1988; accepted 19 April 1989

Temperature Measurements in Carbonatite Lava Lakes and Flows from Oldoinyo Lengai, Tanzania

MAURICE KRAFFT AND JÖRG KELLER

The petrogenesis of carbonatites has important implications for mantle processes and for the magmatic evolution of mantle melts rich in carbon dioxide. Oldoinyo Lengai, Tanzania, is the only active carbonatite volcano on Earth. Its highly alkalic, sodium-rich lava, although different in composition from the more common calcium-rich carbonatites, provides the opportunity for observations of the physical characteristics of carbonatite melts. Temperature measurements on active carbonatitic lava flows and from carbonatitic lava lakes were carried out during a period of effusive activity in June 1988. Temperatures ranged from 491° to 519°C. The highest temperature, measured from a carbonatitic lava lake, was 544°C. These temperatures are several hundred degrees lower than measurements from any silicate lava. At the observed temperatures, the carbonatite melt had lower viscosities than the most fluid basaltic lavas. The unusually low magmatic temperatures were confirmed with 1-atmosphere melting experiments on natural samples.

CARBONATITES ARE IGNEOUS ROCKS rich in primary carbonates, dominantly calcite and dolomite. Although rare compared with silicate rocks, carbonatites provide important constraints on partial melting processes, volatile content, and chemical composition in the earth's mantle.

Oldoinyo Lengai, Tanzania, the only active carbonatite volcano on Earth, is famous for its unusual alkali-rich magma, termed natrocarbonatite. The volcano, a

M. Krafft, Centre Vulcain, F-6700 Cernay, France.
J. Keller, Mineralogisch-Petrographisches Institut der Universität, D-7800 Freiburg, Federal Republic of Germany.